Fall 2016

Construction and validation of TL-IPM generator

Jamaluddin Mohammad

Department:

CONSTRUCTION AND VALIDATION OF TL-IPM GENERATOR

by

JAMALUDDIN MOHAMMAD

A THESIS

Presented to the Faculty of the Graduate School of the

MISSOURI UNIVERSITY OF SCIENCE AND TECHNOLOGY

In Partial Fulfillment of the Requirements for the Degree

MASTER OF SCIENCE

IN

ELECTRICAL ENGINEERING

2016

Approved by:

Dr. Jonathan W. Kimball

Dr. Mehdi Ferdowsi

Dr. Pourya Shamsi

ABSTRACT

Hydrokinetic energy is one of the potential sources of energy that can be extracted and converted to electrical energy using linear generator. This work discusses about construction and validation of tubular linear internal permanent magnet (TL-IPM) generator, a kind of linear generator. The generator could produce electricity by converting linear motion generated from vortex induced vibrations induced due from a flowing fluid, such as a river. A simulation model of the generator is created using Ansoft's Maxwell software, which uses finite element analysis to perform electromagnetic analysis of the generator. Then a practical generator was built and tested. The results of the simulation and experimental generator match each other and predicted behavior. Also a model of the generator has been simulated using Simulink and the performance of the generator was evaluated for various operating conditions. The simulation results were reasonably good and validate that a combination of several generators can be connected together to extract a suitable amount of hydrokinetic energy.

ACKNOWLEDGMENTS

I would like to thank my advisor, Dr. Jonathan W. Kimball, for his constant guidance and encouragement in successfully accomplishing my degree; I would like to express my gratitude for his patience in helping me understand the technical concepts required for the research. I would also like to express my gratefulness to my thesis committee members, Dr. Mehdi Ferdowsi and Dr. Pourya Shamsi, for their valuable contributions and suggestions in my research.

I would like to thank Mathew Gualdoni for his contribution in designing Maxwell model and also I would like to thank Mohammed Alrabiah, Jeremy Johnson, Chris Oleksiw and Ray Peaks, a senior design group, for their contribution in designing the mechanical system. I would like to extend my thanks to Jeff Birt in helping me with all machining work.

This work was supported in part by the MidAmerica Regional Microgrid Education and Training Consortium (MARMET), sponsored by the Department of Energy SunShot program under award DE0006341.

I would like to thank my parents for their support and blessings through my life and for making me a better person today. I would like to express my gratitude to my friends and my fellow lab mates for their constant encouragement throughout this journey.

TABLE OF CONTENTS

Page

LIST OF ILLUSTRATIONS

Page

LIST OF TABLES

Page

1. INTRODUCTION

For the past few decades, the demand for energy has substantially increased. There are various reasons for this such as increase in population, industrialization, standard of living etc. However, this had led to some serious climatic issues such as global warming. For example, 80% of U.S. greenhouse gas emissions are due to the production and use of energy [1]. The growth in energy demand has also resulted in depletion of fossil fuels, resulting in huge energy crisis all over the globe. This has shifted the focus of researchers all over the globe to find alternate sources of energy such as solar, wind, hydropower, bio-fuels etc.

Hydrokinetic energy systems harness energy from the movement of the water like currents, waves or tides [2]. Current applications of hydrokinetic energy have proven to be promising, such as the Pelamis sea "snake" in Portugal, a series of linear generators connected to buoys, which generates 750 kW of electricity [3], and current project proposals suggest that the United States could be producing 13,000 MW of power from applications such as this by 2025, the equivalent of 22 coal power plants [4].

One method of converting the hydrokinetic energy to electrical energy is through a device called linear generator. A linear generator utilizes the translational movement generated by the vortex induced vibrations (VIV) that are produced by a process called vortex shedding [5]. A VIV based generator is considered to be more economical as compared to other renewable sources of energy such as wind, solar etc. [5]. Several different design implementations of linear generators exist, such as flat, tubular, interior or surface-mounted permanent magnet configurations, each with their own benefits [6,8]. The tubular designs tend to exceed the performance of the flat designs due to their radial

symmetry, which minimizes the magnetic leakage and better utilizes the material in the generator [7]. However, the symmetry and close proximity of the stator surrounding the translator does also cause a large cogging force that can degrade performance [9], but the dimensions can be optimized to reduce this effect. A detailed analysis of tubular linear motors with both interior and surface-mounted permanent magnets is given in [10], but little study has been done on optimized generator designs. This thesis discusses in detail about design of an optimized tubular linear generator with an interior permanent magnet. The dimensions of the optimized generator are determined by writing a code in MATLAB [11] using the equations in [10]. A simulation model of the optimized linear generator is developed using Maxwell2D software. The simulation model was modelled to analyse various physical properties like EMF generated, stator inductance, flux linkages and the various forces experienced by the translator. Then a physical optimized linear generator is built in the lab. A mechanical system which could produce linear motion is constructed, to analyse the working of the constructed generator. Finally a simulation model of the designed generator is developed using MATLAB/Simulink to validate the performance of the generator.

2. THEORY

2.1 VORTEX INDUCED VIBRATIONS (VIV)

Vortex Induced Vibrations (VIV) are a periodic motion induced in a bluff body such as a cylinder when an external fluid flows across it. Detailed analysis of extracting hydrokinetic energy from VIV's is explained in [12]. For basic understanding a schematic diagram from [12] is used to explain VIV. Figure 2.1 shows a schematic diagram of a VIV generator module for a single cylinder system.

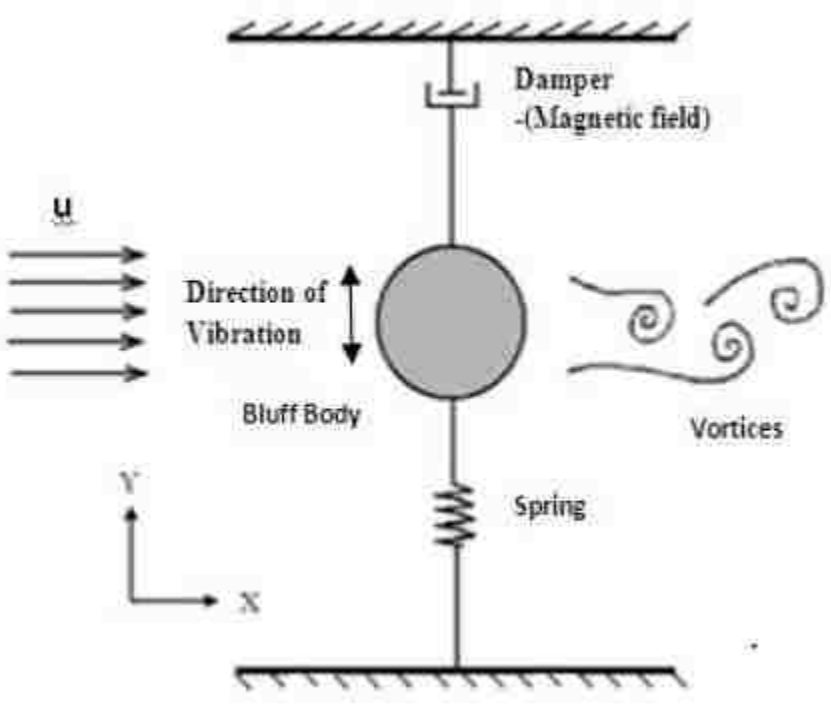

Figure 2.1: A schematic diagram of a VIV generator module for a Single cylinder system[12]

The VIV generator module consists of a cylinder that is coupled with a spring and a damper attached to it. The cylinder is allowed to move only in vertical (y) direction. Whenever the fluid flows across the cylinder a separation of boundary layer begins to take place on the surface of the body. That results in difference of the pressure along the circumference of the cylinder, which causes the cylinder to oscillate. This event is called vortex shedding and the frequency of oscillation is vortex shedding frequency [13]. The amplitude of the vibrations in VIV depends on the mass damping parameter of the system. A system with low mass and low damping will have maximum amplitude [14]. Also the roughness and thickness of the material in which VIV's induced determines the amplitude and frequency response, illustrated in [15] with a series of experiments. The damper may be replaced with a linear generator to extract energy.

2.2 ELECTRO-MAGNETIC ANALYSIS

The process of converting hydrokinetic energy to electrical energy is based on Faraday's law of electromagnetic induction. Which states that change in magnetic field will induce electromotive force (EMF) in a coil through which the magnetic flux passes. Hence mathematically EMF is the rate of change of flux linkage given by equation (1)

$$EMF = -\frac{d\lambda}{dt} \tag{1}$$

Where λ denotes the flux linkage. The negative sign is to ensure the law of conservation of energy and is described by Lenz's law. This law states that the EMF induced by a changing magnetic field must cause a current that will oppose the change in magnetic flux.

Flux linkage λ, is the total flux passing through a closed loop. That means for if a coil has N number of turns then the flux linkage is given by equation (2).

$$\lambda = N\phi \tag{2}$$

Where ϕ denotes the magnetic flux.

The magnetic flux ϕ can be calculated by using equation (3).

$$\phi = \int_S B \bullet dS = \int_S B\cos(\theta)dS \tag{3}$$

Where B is the magnetic field density at the surface, S is the surface area and ɵ is angle between magnetic field lines and the vector normal to the surface.

Hence the amount of induced EMF can be calculated by accurately determining the amount of flux or flux density. This can be determined as follows. To analyze the magnetic field distribution inside the generator a topology of the designed generator is shown in Figure 2.2.

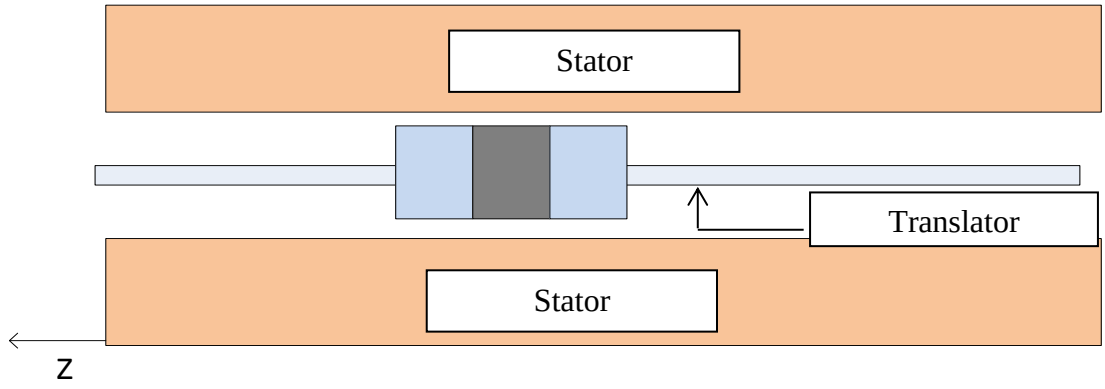

Figure 2.2: Topology of the generator

The translator of the designed generator houses a permanent magnet between two iron discs. There is a small airgap between the permanent magnet and the stator winding. The magnetic field analysis is examined in two regions, viz., the airgap/winding region and the permanent magnet region. Therefore

$$B = \mu_o H \qquad \text{in the airspace/winding} \tag{4}$$

$$B = \mu_o \mu_r H + \mu_o M \qquad \text{in the magnets} \tag{5}$$

Where μ_o, is the permeability of the airgap, $\mu_o \mu_r$ is the permeability of the magnetic region. H is the magnetic field intensity and M is the natural magnetization of the permanent magnet. As the internal tubular section is symmetric and also the permanent magnet is placed axially, the flux density B and magnetic field intensity H will be present in axial direction only. It implies the flux will be linking the stator in axial direction only. Hence there is only one component of B or H to be determined. This is done by defining the magnetic vector potential **A** such that $\mathbf{B} = \nabla \times \mathbf{A}$. Vector **A** is determined by defining various governing field equations and solving them for various boundary conditions which is explained in detail in [16].

3. OPTIMIZED DESIGN

Using primarily equations and findings found in [10], code has been written to optimize the dimensions of a linear generator [11]. From this code, it has been determined that the optimized translator would consist of a permanent magnet with an outer diameter of 19 mm, an inner diameter of 12.7 mm, and a thickness of 9.5 mm. This magnet will be placed between two steel discs of outer diameter 19 mm, inner diameter of 12.7 mm, and a thickness of 3.2 mm. These will all be held centered on a 216 mm long stainless steel rod with collars.

The stator will require a 30.475 mm diameter bore to allow the translator to fit with a sufficiently small air gap. It will consist of six slots for armature windings, each being about 8.43 mm tall and having an inner diameter of 40 mm and an outer diameter of 219 mm. These windings alternate from positive to negative polarity from the top to the bottom of the stator and, in practical application, will be connected in series, as this is a single phase generator. These windings will be separated with 221.075 mm by 221.075 mm steel plates with a 30.475 mm hole to match the cylinder of the stator, and a thickness of 4.12 mm. All of the slots and steel plates will be encased with a top and bottom steel plate of the same dimensions as the previously mentioned plates but with a thickness of 2.06 mm, and spacers will be included to ensure the slots maintain their shape during the construction of the stator. A cross section of the finished generator can be seen in Figure 3.1, with parameters listed in Table 3.1. Note that in Figure 3.1 the gray object is the cross section of the translator, with the permanent magnet in a darker shade of gray, and the blue is the cross section of the stator. The remaining white is the stator bore (airgap).

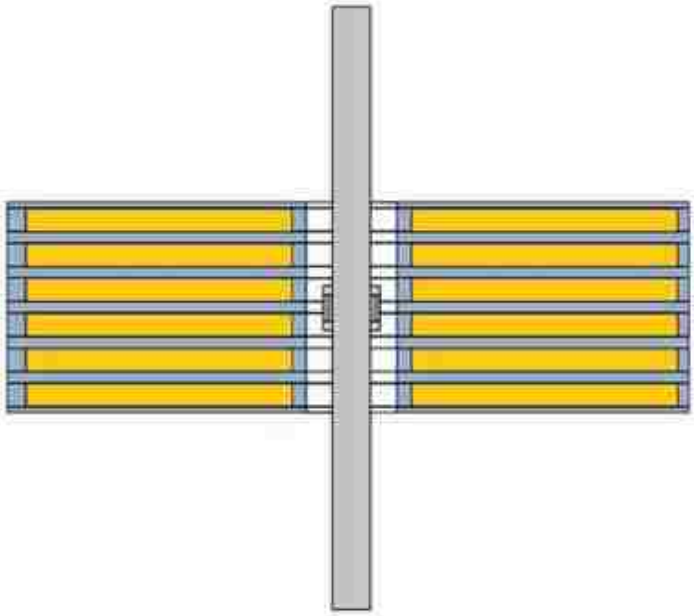

Figure 3.1: Cross-section of the optimized linear generator

Table 3.1: Optimized dimensions of the linear generator model

Translator	
Stainless Steel Shaft	
Diameter	12.7 mm
Length	19 mm
Permanent Magnet	
Outer Diameter	19 mm
Inner Diameter	12.7 mm
Thickness	9.5 mm
Plate Thickness	3.2 mm

Stator	
Outer Diameter	219 mm
Inner Diameter	30.475 mm
Teeth Thickness	4.12 mm
Top/Bottom Plates	2.06 mm
Winding Slots	
Inner Diameter	40 mm
Outer Diameter	219 mm
Thickness	8.43 mm

4. SIMULATION MODEL

The optimized tubular linear generator has been modeled in Maxwell2D, a program that uses finite element analysis to solve electrostatic, magnetostatic, eddy current, and transient problems. Due to the symmetry of the model around the z-axis, a two-dimensional analysis will be sufficient. To determine the behavior of the generator, different simulations were run and several post-processing tools of the program were utilized. This section will detail the setup of the model as well as the simulations to determine the detent forces experienced by the translator due to reluctances in the system, the inductance of the stator due to the coil windings, and the EMF generated by the movement of the translator.

The first thing to note is the mesh operations that define how the program solves for the values detailed in the following pages. The simulation model is broken up into finite elements to simplify calculations. Mesh operations define how the elements should be formed. For this model, a length-based mesh operation was selected, which sets a maximum length of a side of a mesh as well as a maximum number of elements the selection can divided into. To ensure the magnetic field generated by the permanent magnet is computed accurately, the mesh operation for the edge of the magnet has been set for a maximum length of 0.33 mm and a maximum of 500 elements. The stator is set to have several mesh operations, with some covering different portions of the stator to encourage symmetry within the mesh. The mesh operations on the edge of the stator have a maximum length of 2 mm while the inside mesh operations are set to 5 mm, all restricting the number of elements to 1000. The top and bottom of the stainless steel rod

both have edge based mesh operations 20 mm with 1000 maximum elements. The mesh plot constraints for the model can be observed in Table 4.1 with the plot in Figure 4.1.

Table 4.1: Mesh operation constraints

Stator	
On Edge	
Max Length	2 mm
Max Elements	1000
Inside	
Max Length	5 mm
Max Elements	1000

Permanent Magnet	
On Edge	
Max Length	0.33 mm
Max Elements	500
Stainless Steel Shaft	
Inside	
Max Length	20 mm
Max Elements	1000

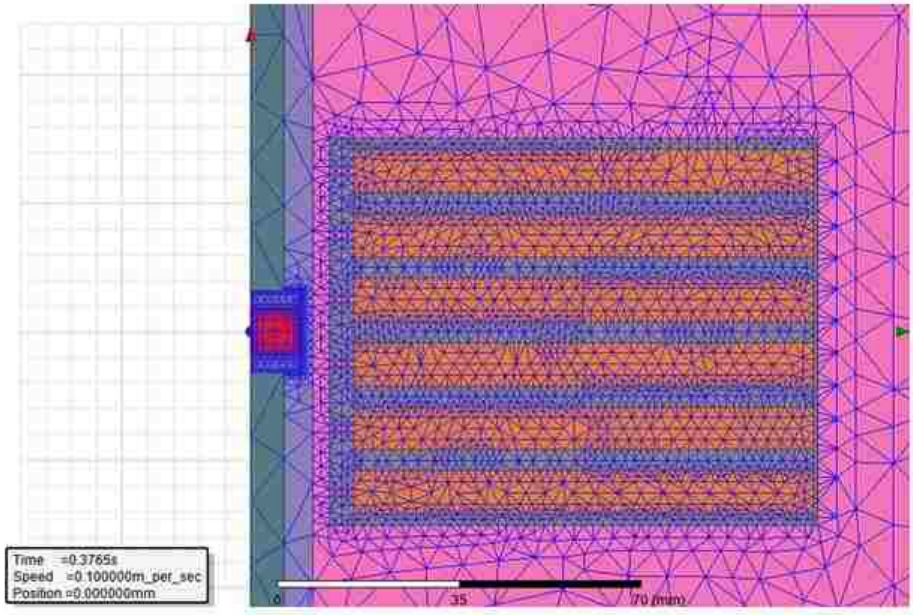

Figure 4.1: Mesh plot for the simulation model

5. SIMULATION RESULTS

Initially the simulation program was setup to solve for a transient magnetic solution. The translator moves through the generator (the permanent magnet going from -37.65 mm to 37.65 mm, relative to the center of the stator on the z-axis) at a constant velocity of 100 mm/s with no current running through the stator windings to observe the system with no magnetic fields present aside from the field generated by the permanent magnet. The average flux density through the center of each plate was computed to verify that the model was symmetric, and can be observed in Figure 5.1. Note the graph is mirrored across the 0 mm point, showing the model is, in fact, symmetrical.

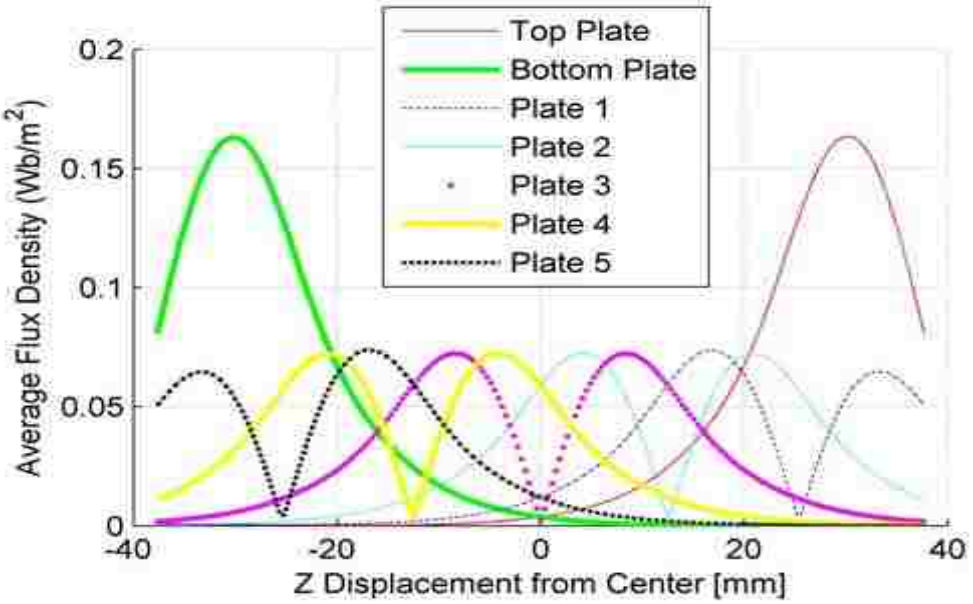

Figure 5.1: Average flux densities through steel plates

The actual (local) flux density needs to be examined as well to determine how close to saturation the generator might be. The flux density contour can be seen in Figure 5.2 for the position with the permanent magnet centered and in its final position.

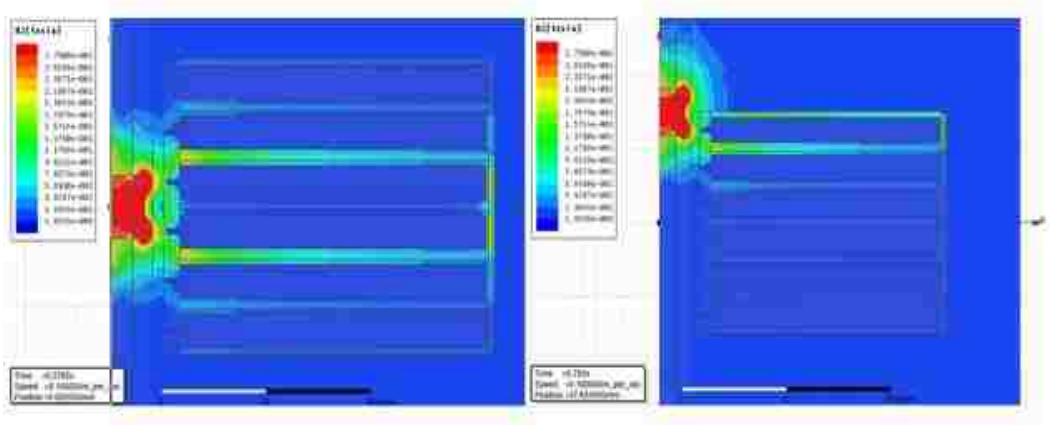

Figure 5.2 : Flux density of the system, with the PM centered in the stator on the left and in its final position on the right

As flux passes through the path of less reluctance this behavior is expected from this generator; copper is a non-ferromagnetic material, so its relative permeability, like air, is close to unity, whereas steel 1008 has a relative permeability on the order of 1000 in the presence of a magnetic field up to 1 T. This explains why the flux contour shows a majority of the magnetic flux going through the steel in the stator as opposed to the copper. Examining the flux density, only a small portion of the generator approach 275 mT. Referencing the hysteresis curve in Figure 5.3 it is clear that this is far below the

saturation point; significant changes in the magnetic permeability do not occur until roughly 1.5 T, therefore losses present in the system are minimal.

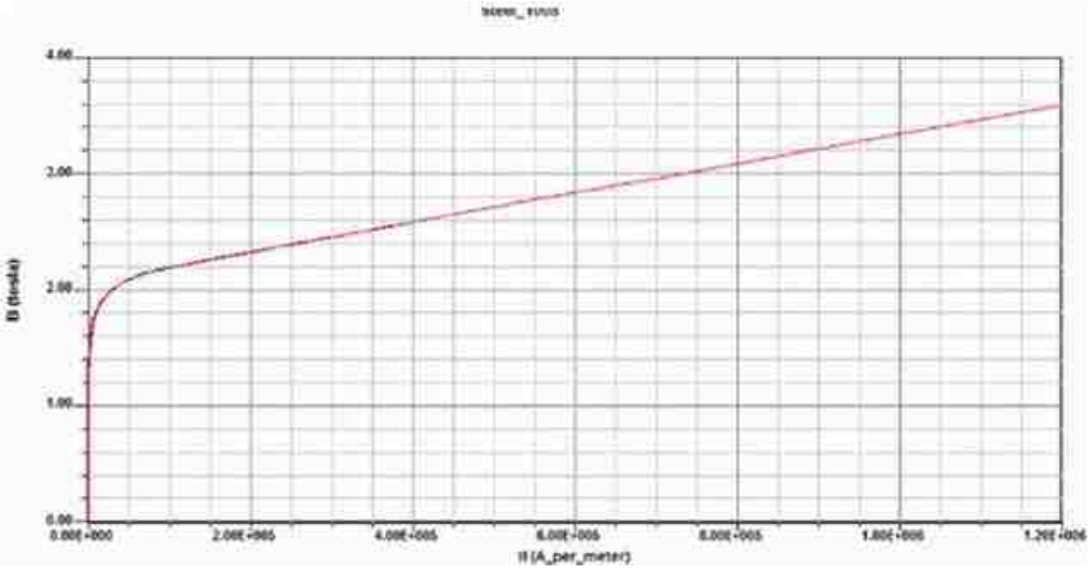

Figure 5.3: Hysteresis curve of steel 1008 [17]

Since no current is flowing through the windings, no magnetic field is being generated to oppose the movement of the translator. This allows the cogging force, the force on the permanent magnet due to the reluctances in the stator, to be determined. This force can be viewed in Figure 5.4 the x-axis is a measurement of the displacement of the center of the permanent magnet relative to the center of the stator. Due to the symmetry of the system, all tangential forces cancel out, leaving only a force acting along the z-axis. Note that the force is minimal when the translator is entirely within the stator. This is due to the effect of the permanent magnet transitioning from a point outside the stator,

where much of the flux is in the surrounding vacuum, to inside the shaft of the stator, where low reluctance paths are present.

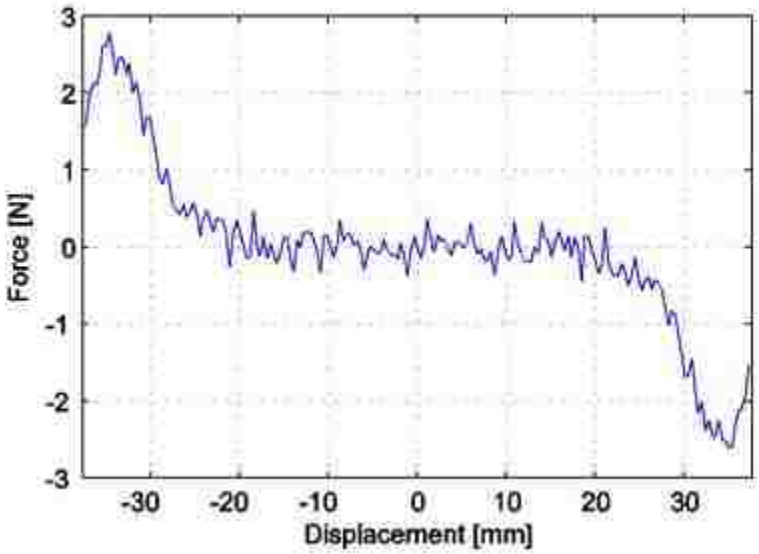

Figure 5.4: Reluctance force on permanent magnet due to stator

From the flux linkage data, the generated EMF can be obtained by approximating the derivative of the flux linkage of the system with respect to time. This is done by finding the difference between adjacent values and dividing the new data by the sampling time. Another method to obtain a smoother plot is to use a sliding-window averaging approach. This was done by fitting a linear equation to a number of data points and taking the derivative of each line to give the approximation; after performing this approximation for different numbers of points, five points per linear approximation seemed to be an appropriate number. These approximations, as well as the induced voltage computed by

Maxwell2D, can be seen in Figure 5.5, which is the no-load case with 100 mm/s movement by the translator. The approximations fit the curve computed by the modelling software, with a slight phase shift. This phase shift is likely do to some interpolations within the position vector to account for the changes in the inductance data vector. For example, using the sliding-window averaging approach, the inductance data vector will be four samples smaller than the position vector, requiring a new position vector to be created to plot the data.

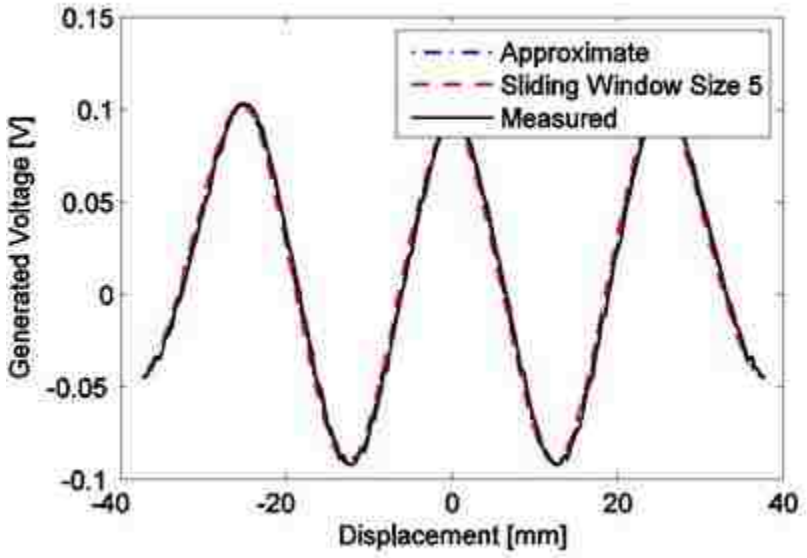

Figure 5.5: Voltage generated (measured and approximated)

Next, the inductance of each coil was measured to observe how the inductance of the system behaves with respect to the position of the stator. This data can be seen in

Figure 5.6, and is symmetric as one would expect. Since the windings will be connected in series in practical application, the overall inductance can be computed by adding all of the inductance plots together. This yields the graph seen in Figure 5.7. Note that the inductance is maximum when the translator is within the stator, but not centered. This is further evidence of the canceling effect of the windings. When the translator is closer to one end of the stator, all coils are experiencing different levels of flux linkage. Cancellation still occurs, however the coil closest to the permanent magnet exhibits the strongest flux linkage, and therefore dominates the flux linkage of the system. This explains why the magnitude of the linkage is at a maximum near the ends of the stator as shown in Figure 5.4. Because the linkage is near the peak, the change in flux linkage is relatively small compared to the changes experienced in other positions within the stator. This is reflected in the inductance of the system.

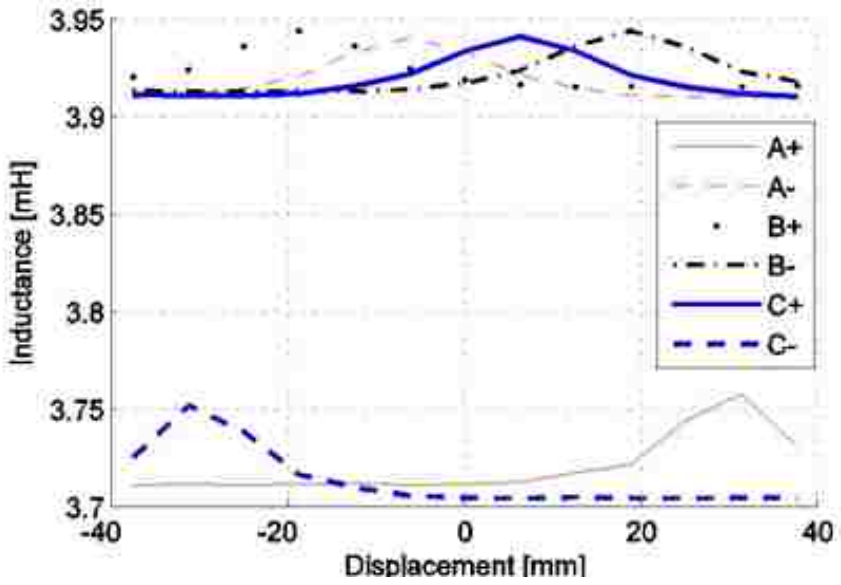

Figure 5.6: Inductance due to each coil related to the position of the translator

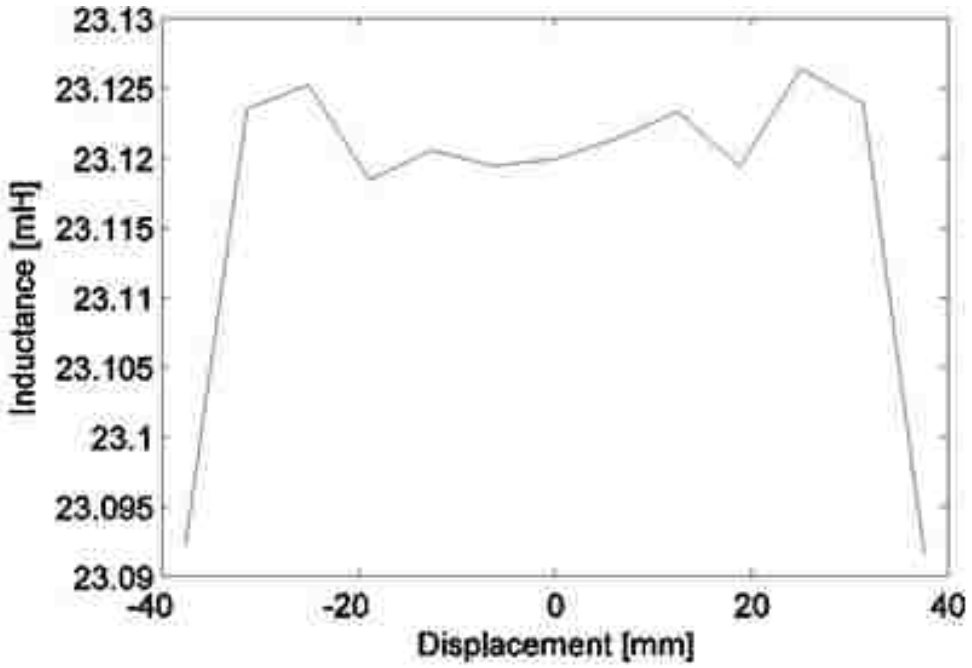

Figure 5.7: Inductance of the system as measured by the simulation software

To determine how the inductance of the system was affected by the armature current, a magnetostatic simulation was run with the translator centered in the stator. The current through the armature windings was then swept from -10 A to 10 A in steps of 200 mA. The simulation software recorded the flux linkage data for each of the windings, which were then summed to give the overall flux linkage as a function of current. The derivative of this data must be approximated, and since is the data are very nearly linear (see Figure 5.8), the sliding-window technique was used again. The resulting curve is Figure 5.9, with several different window sizes shown. Notice that the inductance near 0 A is close to 21 mH, which is only a few millihenries away from what was measured in the transient solution as shown in Figure 5.7. However, as more current is placed in the

armature windings, the magnetic fields generated by the current cause the system to become more saturated.

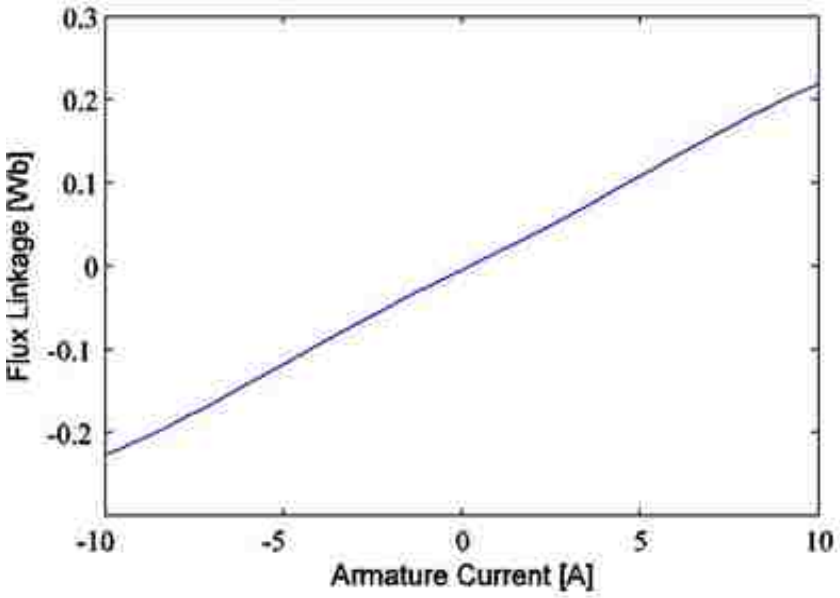

Figure 5.8: Flux linkage of the system

As mentioned previously, as the magnetic field density induced in the stator increases, the magnetic permeability, and thus the magnetic permeance, decreases. This should result in system inductance being at a maximum when there is no current in the armature windings and gradually decreasing as the current increases, however this is not the behavior exhibited by the simulation model. This inconsistency with expectations might be attributed to how the simulation software solves a magnetostatic problem as opposed to transient problems.

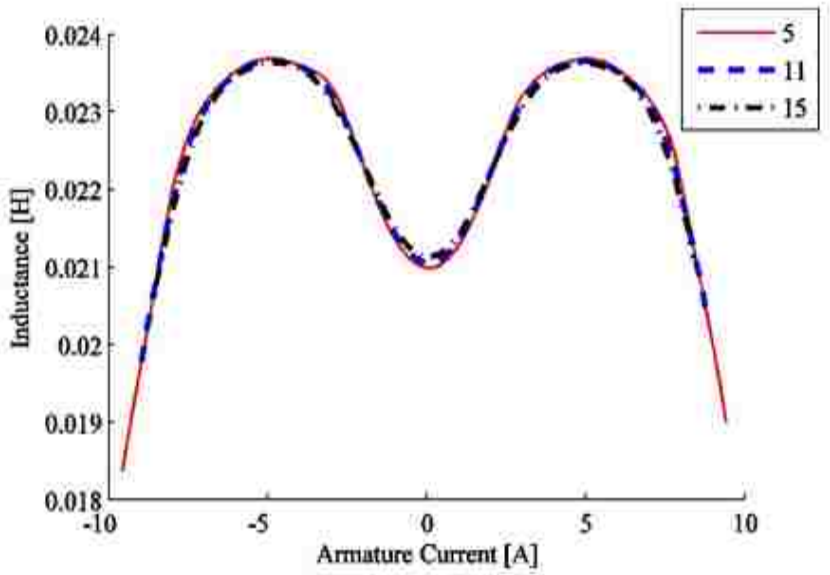

Figure 5.9: Approximate inductance of the system

To obtain a more complete set of data, another transient simulation was run with thirteen samples, meaning samples are taken at each end of the stator, the center of the stator, in the center of each coil winding, and in between all adjacent windings as well, from 0 A to 10 A in steps of 200 mA. Using this dataset, the generator can be modeled in Simulink in MATLAB. Given an armature current input and a position for the translator, the program can interpolate a value for the flux linkage of the system for the given conditions. From this, the program can calculate the generated voltage, allowing for simpler software simulations to be run in the future to further analyze the expected performance of the generator.

Lastly, practical power outputs are observed for the translator moving 100 mm/s. According to [8], acceptable forces for this application will be between 1.4 and 1.6 N. Using the transient simulation data, the armature current values that cause the permanent

magnet to experience a force less than 1.6 N can be isolated and used to determine a power plot. However, since the translator experiences a greater force near the edges of the stator, an assumption is made that the translator will stay within the stator. Specifically speaking, the first two and last two samples taken are ignored.

Once these currents are determined, the voltage values are stored in an array, and then each dataset is multiplied by the proper armature current. The resulting graph can be viewed in Figure 5.10.

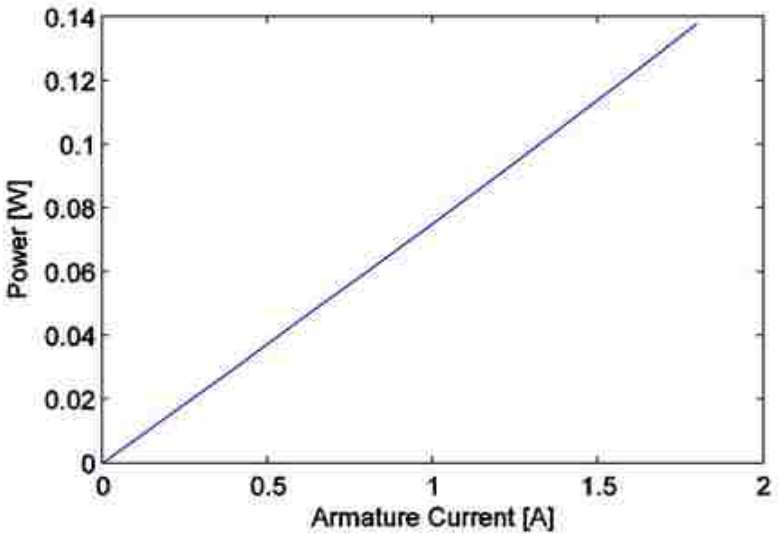

Figure 5.10: Potential power outputs for the plausible armature currents that can be obtained with the translator moving at 100 mm/s

These voltages are not insignificant, and several generators can be connected in series to obtain a desired voltage for a specific application. This will be where the Simulink model will become useful; depending on the voltage and the current

requirements for the application, a configuration of strings of linear generators in series with the strings connected in parallel can supply a larger amount of current and a greater voltage for the application.

6. PRACTICAL LINEAR GENERATOR

This section explains about the construction of the linear generator, mechanical system to generate linear motion and testing of the linear generator

6.1 CONSTRUCTION OF THE LINEAR GENERATOR

A practical linear generator of dimensions obtained in the optimized linear generator code [11] is built in the lab. The stator consists of six square shaped steel frames of dimensions 2210.75 mm by 221.075 mm with thickness of 13 mm. Each frame is made of several thin laminations of steel plates stacked together. Basically there are two structures of steel plates as shown in Figure 6.1.

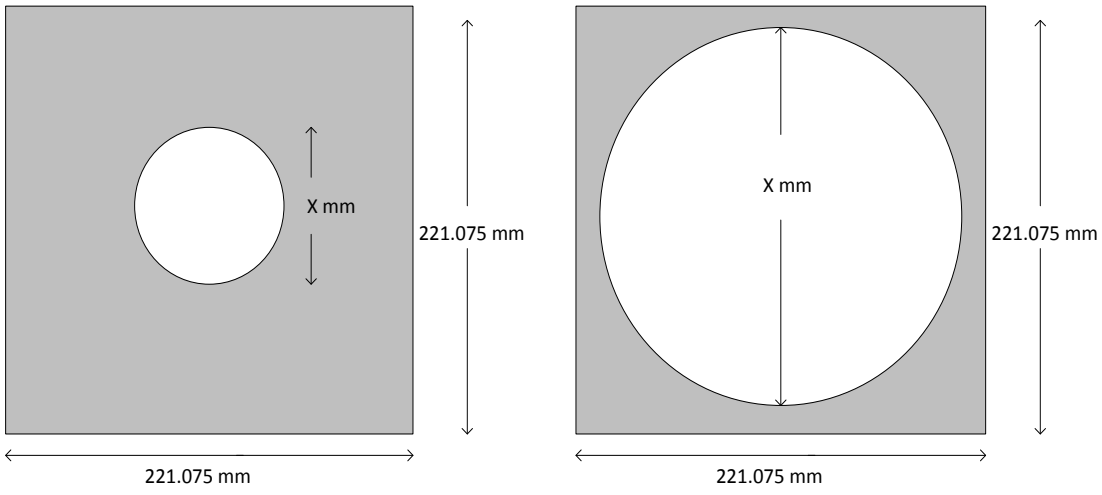

Figure 6.1: Stator laminations

One has a central hole of 30.475 mm as shown in Figure 6.1(a). When all the frames are stacked together, this hole forms a cylinder to accommodate the rotor. This plate forms the base of every stator frame. The other plates have a hole of 198.05 mm as shown in Figure 6.1(b). When these plates are stacked together on top of the base plate, a pocket is formed where the stator winding is placed. All these steel plates are attached to each other by seam welding them. The slots in the stator are wound with a 25 AWG copper wire. The armature windings are winded in a circular fashion with approximately 1100 number of turns in each stator frame. To accommodate maximum amount of copper wire it was made sure that the windings are tight and close to one another without leaving much air gap. Kapton tape was used to at regular intervals (approximately at every 100^{th} turn) to keep the winding held tight and attached to the stator frame. Figure 6.2 shows a picture of the stator frame with armature winding.

Figure 6.2: Stator frame with armature winding

These six stator frames are separated from one other using a steel plate of same dimension of the stator frame lamination and then stacked together using nut and bolt at all the four corners of the stator. The hole in the center of the stator laminations forms a cylinder of diameter 30.475 mm across the stator. This cylinder houses a permanent magnet rotor or the translator. An axially magnetized ring shaped permanent magnet with 19 mm outer diameter, 12.7 mm inner diameter and 9.5 mm thickness from K&J magnets is used. This magnet is held centered on a 216 mm stainless steel rod with two steel discs of outer diameter 19 mm and inner diameter 12.7 mm on both sides of the magnet. The steel discs will direct the flux through the generator. Figure 6.3 show the rotor with the permanent magnet and the Figure 6.4 shows the assembled linear generator.

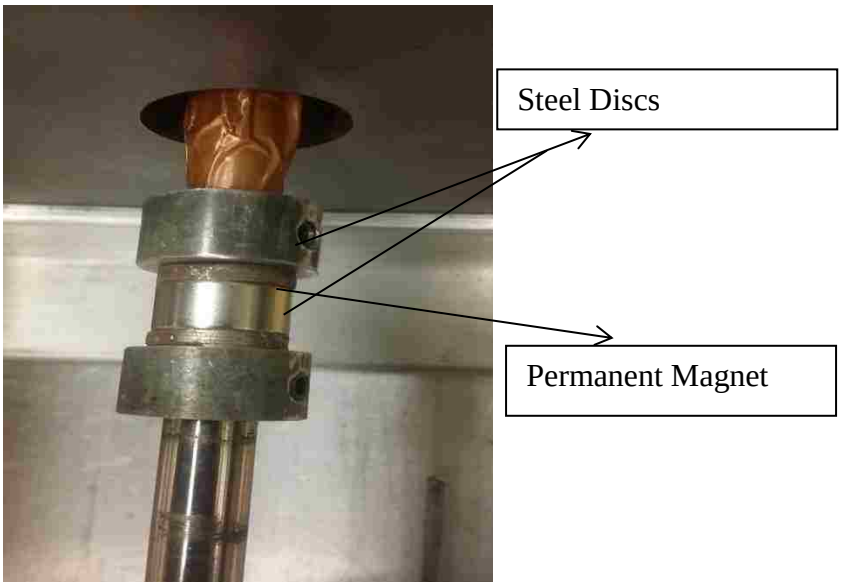

Figure 6.3: Translator of the Generator

Figure 6.4: Assembled linear generator

6.2 MECHANICAL SYSTEM

A mechanical system capable of producing linear motion is built in the lab. This linear motion is assumed as the linear motion produced by the VIV's and hence used to drive the rotor of the generator. The mechanical system is basically a crank-shaft mechanism driven by an induction motor rated 0.5 HP. A variable frequency drive Yaskawa A 1000 model is used to operate the induction machines at various different speeds. The motor and drive set is shown in Figure 6.5.

Figure 6.5: Motor with VFD

The shaft of the induction motor is connected to a steel crankshaft as shown in Figure 6.6, with a crank length of 4.5 in. Hence the stroke length is 9 in., which is sufficient to drive the permanent magnet of the translator from one end of the stator to the other end.

Figure 6.6: Crankshaft

The crankshaft is supported by two roller bearings and coupled to a wooden connecting rod as shown in Figure 6.7. The crank shaft and connecting rod mechanism converts the angular motion generated by the induction motor to a linear motion.

Figure 6.7: Connecting Rod

A connecting rod is attached to the translator/rotor of the generator. This translator is supported by an air bearing system, fueled by an air compressor at 60-70 psi. On the other end of the translator a Fagor linear encoder, model #MOX-375 is attached to measure the position and velocity of the translator. Figure 6.8 shows the linear encoder. Linear generator is coupled with the mechanical set up to test the performance of the generator. Figure 6.9 shows the experimental set up of the linear generator with the mechanical system.

Figure 6.8: Linear Encoder

Figure 6.9: Linear Generator coupled with Mechanical system

7. TESTING AND RESULTS

7.1 VOLTAGE MEASUREMENT

The designed generator is assembled with the mechanical system. Then the induction motor is operated at very low speed by setting the frequency of the drive at 2 Hz. Voltage across each stator winding is measured is measured using a Tektronix MSO4054 oscilloscope. Figure 7.1 shows the voltage across the first four plates of the stator; channel 1 shows the voltage across winding in stator plate 1 channel 2 across plate 2 channel 3 across plate 3 and channel 4 across plate 4. There is a phase shift between the voltages of the four windings because of the relative position of the permanent magnet.

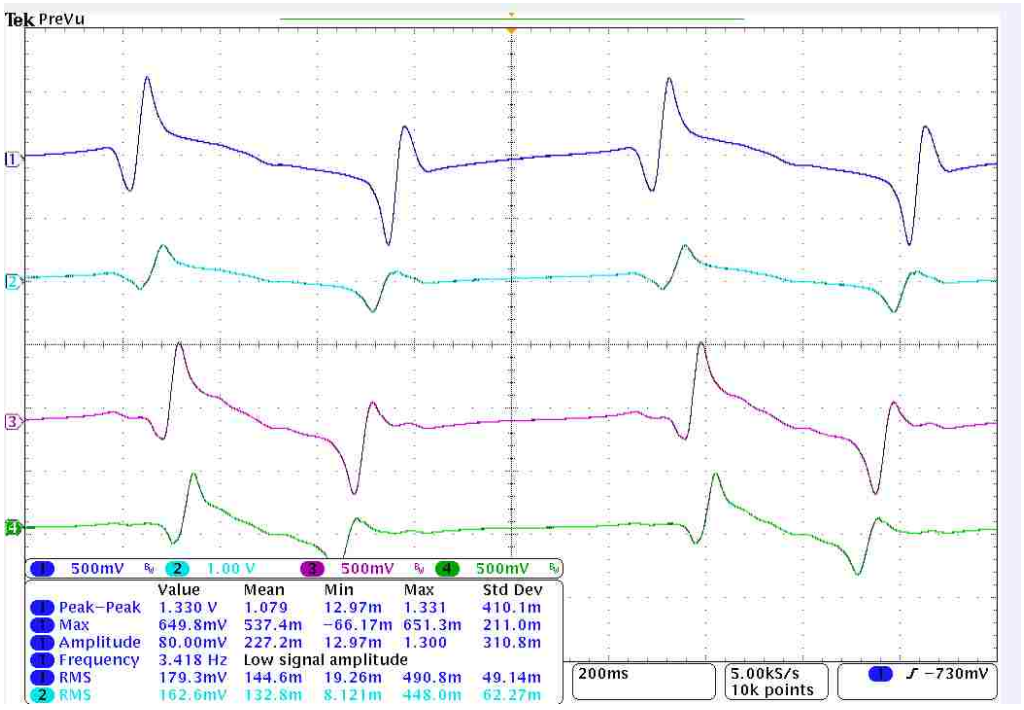

Figure 7.1: Voltage across each stator winding

All the six stator windings are connected in series so that the total voltage would be the sum of the individual coil voltages. The voltage across the end terminals of the series connected stator is measured as shown in Figure 7.2. The measured voltage is quite similar to the voltage obtained from the Maxwell simulation. However, the voltage peaks in all the six windings are not same as each other as would be expected. This is most likely due to the fact that the number of turns in all the frames is not equal, as the winding was done manually.

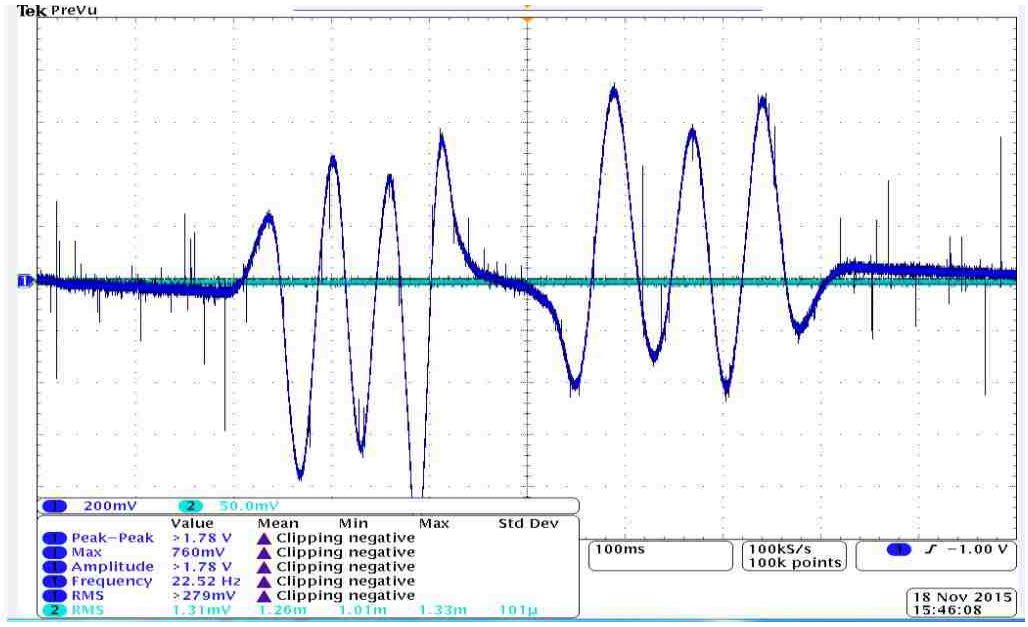

Figure 7.2: Terminal voltage with no load at 2 Hz

To obtain maximum power transfer, a resistive load of 310 Ω (equal to the internal resistance of the generator) is connected at the end terminals of the generator.

Voltage is measured for loaded condition keeping the translator speed unchanged from the no load condition. As seen in Figure 7.3 voltage under the loaded condition looks similar to the No-load condition, except at a lower magnitude because of the voltage drop in the stator windings.

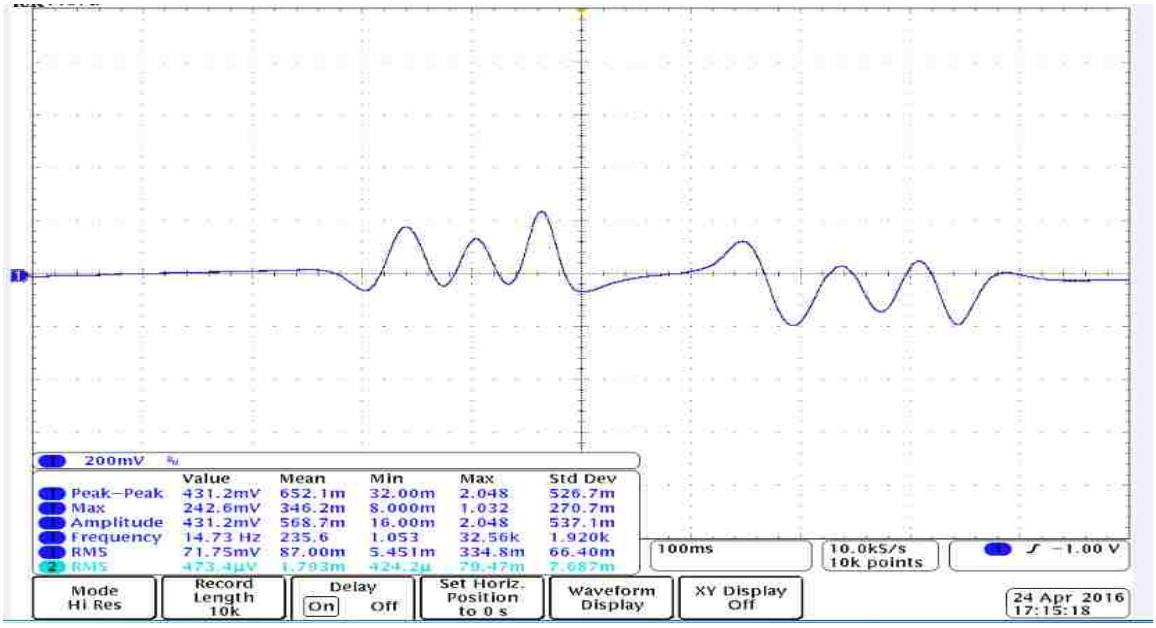

Figure 7.3: Terminal voltage with load at 2 Hz

Now, the drive is set to operate at 4 Hz, double the initial speed. The voltages under no load and full load are obtained as shown in Figure 7.4 and 7.5 respectively. As the speed of the translator is almost doubled, the voltage at no load is almost doubled. However, during loaded condition the voltage is somewhat lesser than the twice the voltage obtained at 2 Hz because with increase in speed, the armature current also increases hence more voltage drop across the stator winding.

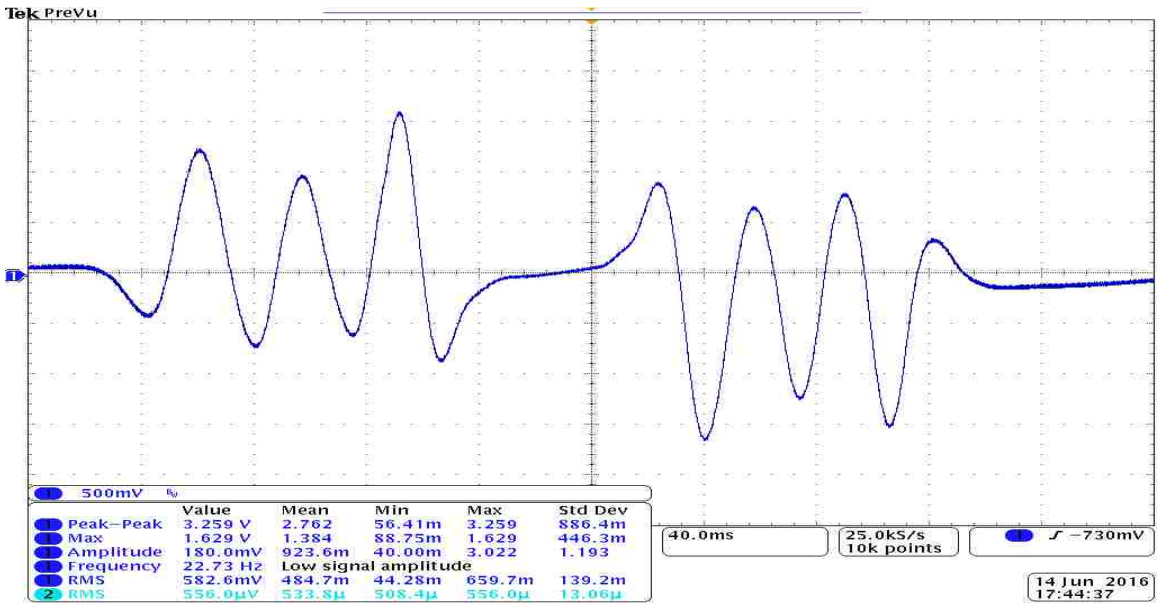

Figure 7.4: Terminal voltage at No- load at 4 Hz

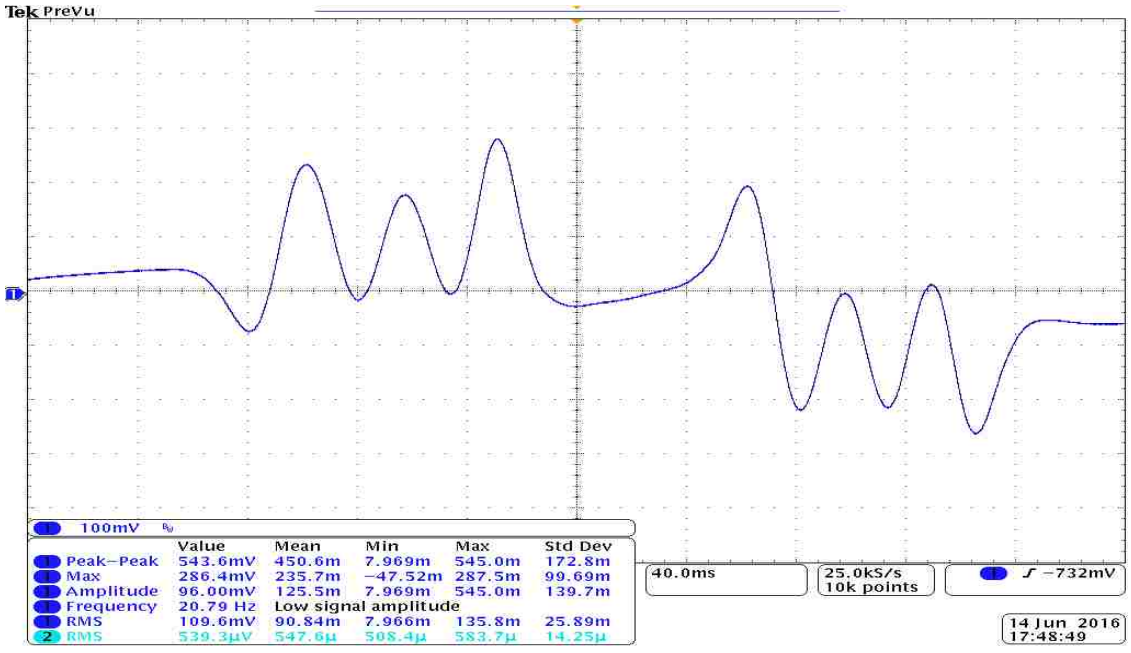

Figure 7.5: Terminal voltage with load at 4 Hz

7.2 POSITION MEASUREMENT

The relative position of the translator is measured using a Fagor linear encoder. Position is measured so that relation between voltage and relative position of the translator can be derived. Fagor #MOX-375 is an incremental linear encoder which has a graduated glass material with 20 micron etching pitch. It has reference marks at every 50 mm of distance. It uses optical transmission to measure position. It has an LED at one end and the photo diode at another. The light from the LED goes through an engraved glass and then reaches photo diode. Which generates electrical signals of period same as the graduation pitch. These electrical signals are carried over a cable attached to the linear encoder. By counting the number of pulses received, the relative position may be measured. Linear encoder has an accuracy of 5 μm and resolution of 1 μm.

A LabVIEW program is used to decode the electrical signals and measure the position. The electrical signals from the encoder are interfaced to LabVIEW using DAQ card .The pin out configuration is shown in Figure 7.6. Pin 12 and pin 10 of the encoder are connected to pin 12 and pin 35 of the DAQ card respectively; this provides 5 V supply for the encoder. Pin 5 and pin 8 of the encoder are connected to pin 42 and pin 46 of the DAQ card; these pins carry the generated electrical signals from the encoder. Figure 7.7 shows a screenshot of the LabVIEW program that decodes the electrical signal generated by the encoder and converts them into distance by counting the number of pulses of the electrical signals. The distance is displayed using a waveform chart as shown in Figure 7.8.

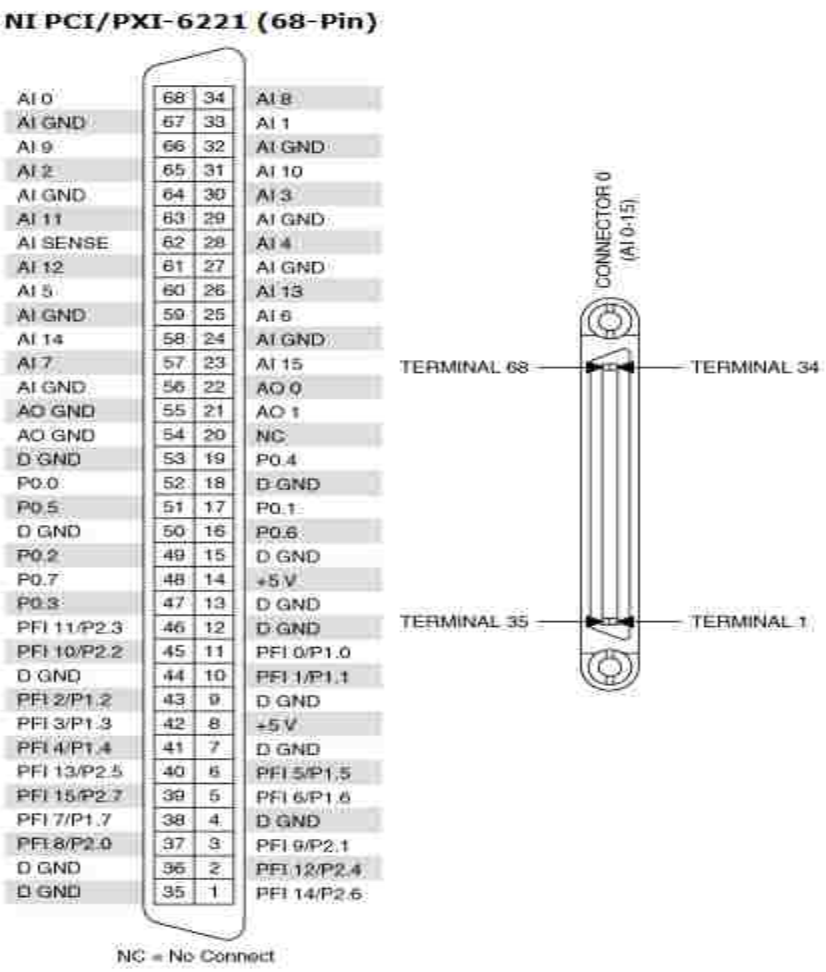

Figure 7.6: Pin configuration of DAQ card

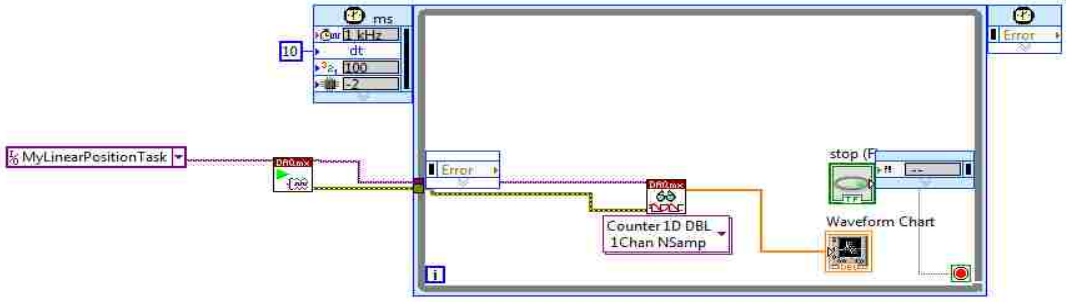

Figure 7.7: LabVIEW program to measure position

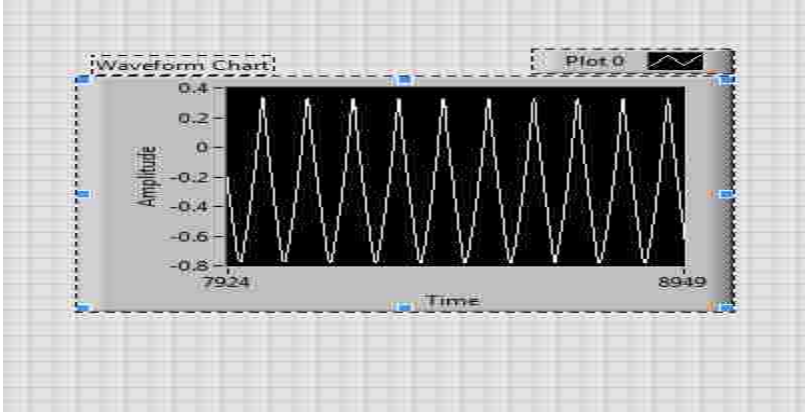

Figure 7.8: Position measured

To further validate the performance of the generator, the practical position and voltage data obtained has been used to find the change of flux with respect to the position and compared with the simulation results. Change of flux with respect to position with respect to position is obtained mathematically as shown below.

EMF generated e = change of flux w.r.t to time= $\frac{d\lambda}{dt} = \frac{d\lambda}{dx} \bullet \frac{dx}{dt}$

$$\Rightarrow \frac{e}{\frac{dx}{dt}} = \frac{d\lambda}{dx}$$

where $\frac{dx}{dt}$ is velocity, obtained by finding a derivative of the distance/position.

The practical results closely match the simulation, as shown in Figure 7.9 The experimental graph is jagged because of a shortage of points, due to the limited time resolution of position measurements in LabVIEW.

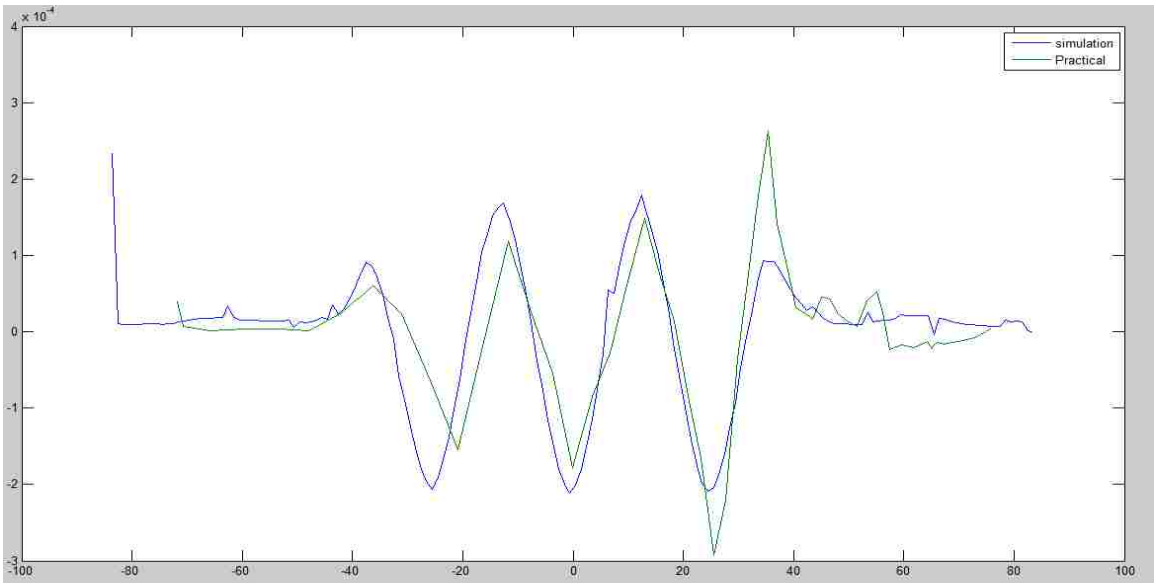

Figure 7.9: Change of flux with respect to position

8. SIMULINK MODEL OF THE GENERATOR

8.1 SIMULATION MODEL

A simulation model of the linear generator is built using MATLAB/Simulink. This model will compute the output voltage and power produced for a given position profile. Figure 8.1 shows the Simulink model of the generator.

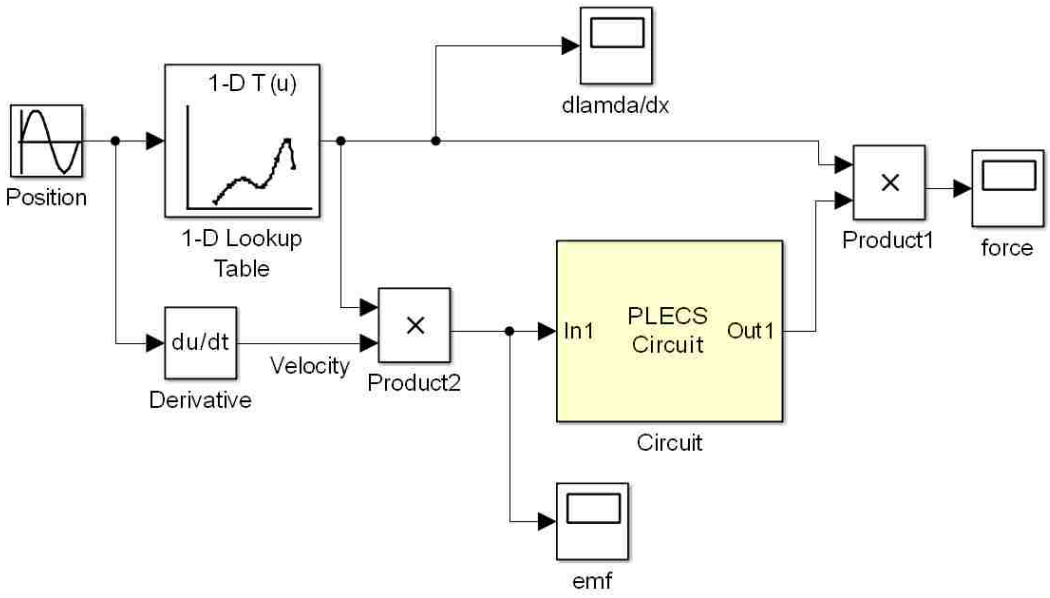

Figure 8.1: Generator Model

The 1-D lookup table computes the change of flux with respect to position ($\frac{d\lambda}{dx}$), for a given position profile. Internally, the 1-D lookup table uses the data of change of

flux with respect to position obtained from actual physical generator to compute $\frac{d\lambda}{dx}$ for any given position profile. Then $\frac{d\lambda}{dx}$ is multiplied with velocity, obtained by derivation of position, to compute the EMF produced. EMF is fed as input to the PLECS circuit, internal of the PLECS circuit is shown in Figure 8.2. R1 and L1 are the internal resistance and the inductance of the generator. R2 is the load resistance whose value is equal to internal resistance R1 for maximum power transfer.

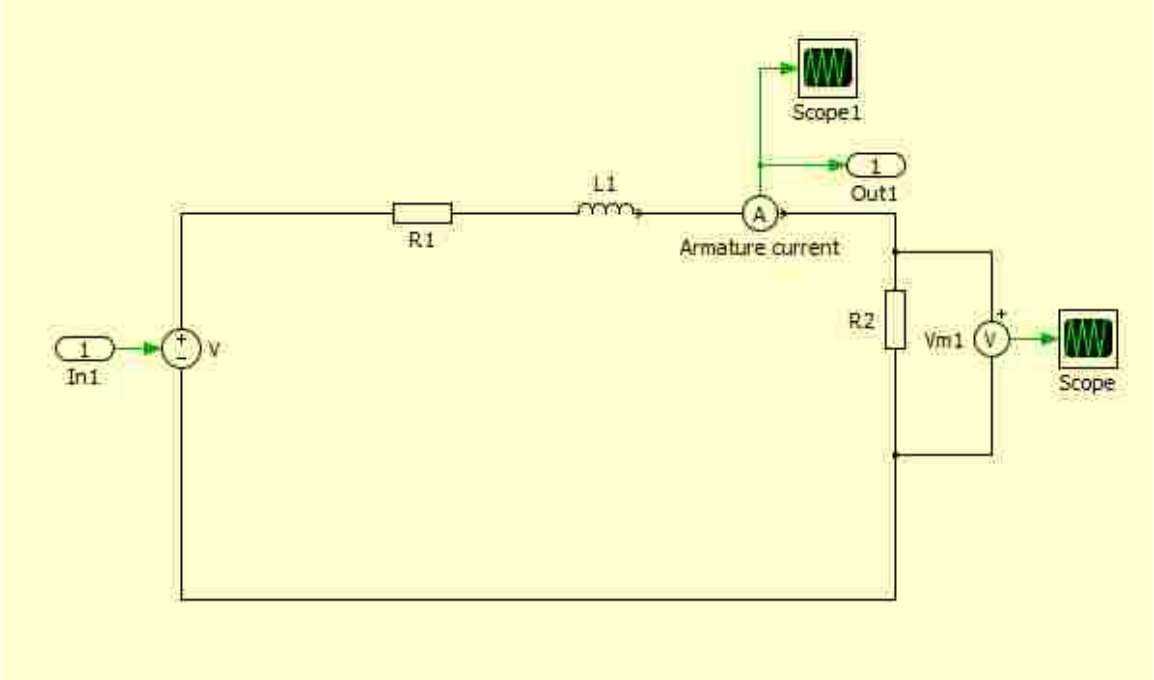

Figure 8.2: Internal of PLECS circuit

Armature current is multiplied with $\frac{d\lambda}{dx}$ to compute the force. In the future a mechanical system can be attached to this model, so that for a given force and position

from a mechanical system the generated voltage/ power from the linear generator can be computed. Hence the model can be used to evaluate the performance of the generator for a given mechanical input variables.

8.2 SIMULATION RESULTS

The simulation model of the linear generated was tested for various conditions detailed as below.

Case-1: Full stroke length, speed =2 Hz

In this case the generator model is considered for full stoke length that means the permanent magnet on the translator will completely come out of the stator tube. And the speed of the translator is set at 2 Hz. Simulation time is set such that the translator completes one full cycle, that is, one forward stroke and one backward. For these conditions the output voltage, power and force waveforms are shown in Figures 8.3, 8.4 and 8.5 respectively.

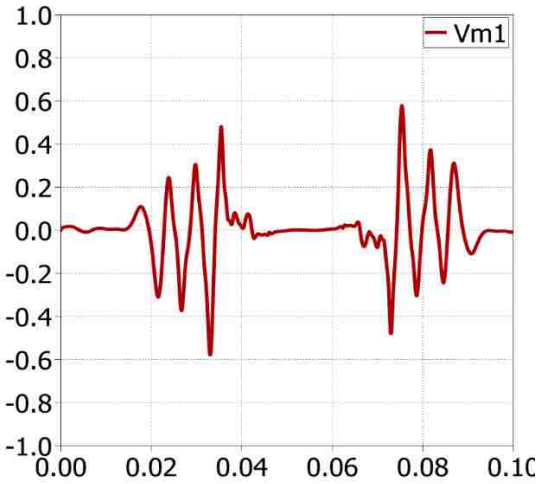

Figure 8.3: Terminal Voltage at 2Hz Full stroke length

The terminal voltage shown is for one complete cycle, i.e., one forward stroke and one backward. The voltage waveform quite matches with the practical results. During the time interval between forward and reverse stroke the voltage is zero, due to the fact that magnet is completely outside of the stator during this time interval. Similar behavior is observed in power waveform; also the output power is very small as the voltage and current are very small. As the load resistance is equal to the internal resistance it is the maximum power that could be extracted from the generator for the above operating conditions.

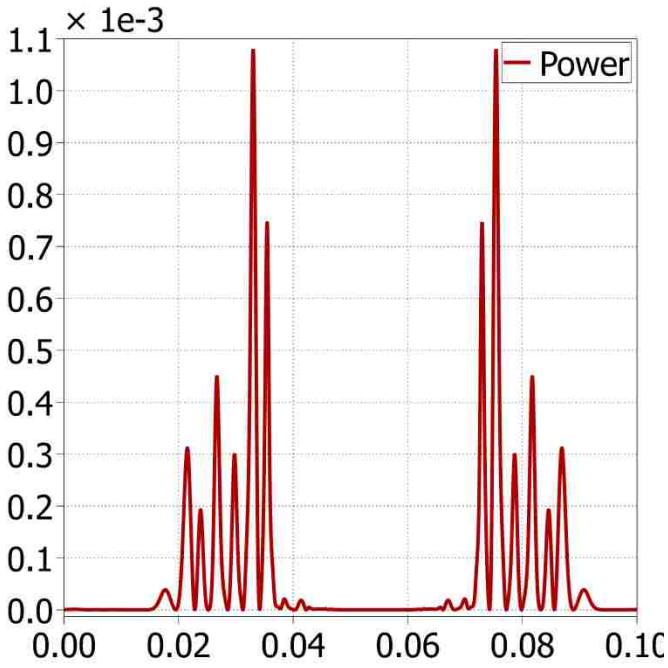

Figure 8.4: Output Power at 2Hz Full stroke length

The mechanical force on the translator as shown in Figure 8.5 is very small because of the fact of very little power is produced from the linear generator. Force changes its direction during reverse stroke as the translator travels in the backward direction during reverse stroke.

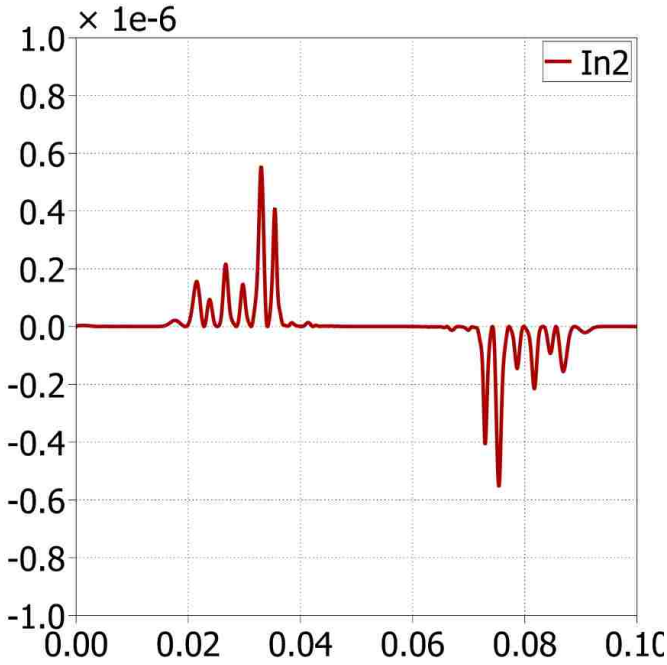

Figure 8.5: Force at the translator 2Hz Full stroke length

Case-2: Reduced stroke length, speed =2 Hz

In this case the generator model is considered for a reduced stroke length such that the translator will stay inside the stator tube. And the speed of the translator is set at 2 Hz. Simulation time is set such that the translator completes one full cycle, that is, one

forward stroke and one backward. For these conditions the output voltage, power and force waveforms are shown in Figure 8.6, 8.7 and 8.8 respectively.

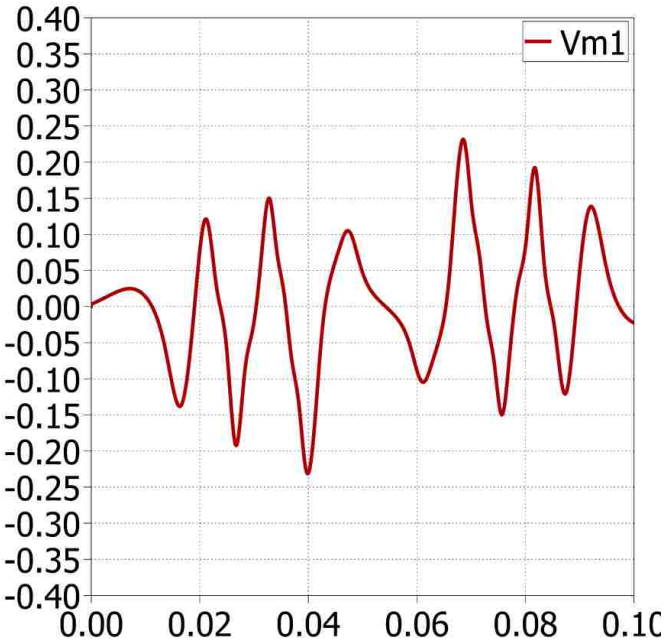

Figure 8.6: Terminal Voltage at 2Hz reduced stroke length

As the translator stays inside the stator tube the voltage will not go to zero. The reverse stroke voltage follows immediately after the forward stroke. Also the amount of voltage got reduced because with reduced stroke length the velocity is reduced eventually resulting in reduced voltage. Also the amount of power is reduced with a smaller stroke length. In this case the stroke length is almost reduced by half as compared to case -1, hence power is reduced by almost four times as both voltage and current reduced by half.

Similarly the force waveform does not have the zero force time period. Also the amount of force decreased with a lesser stroke length.

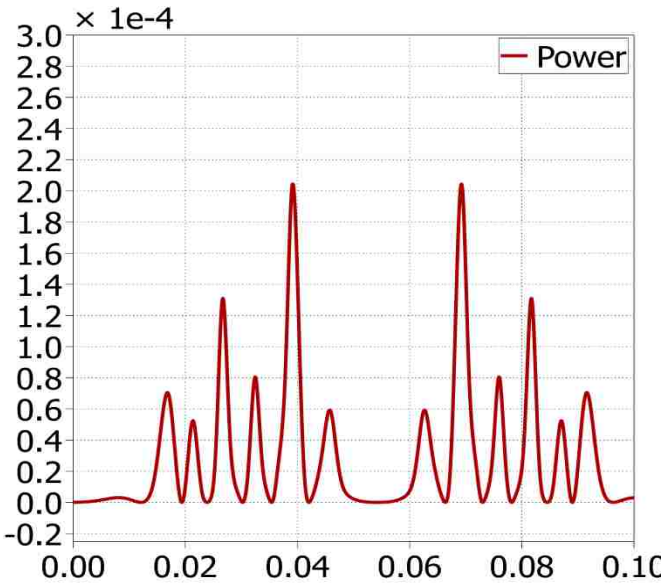

Figure 8.7: Output Power at 2Hz reduced stroke length

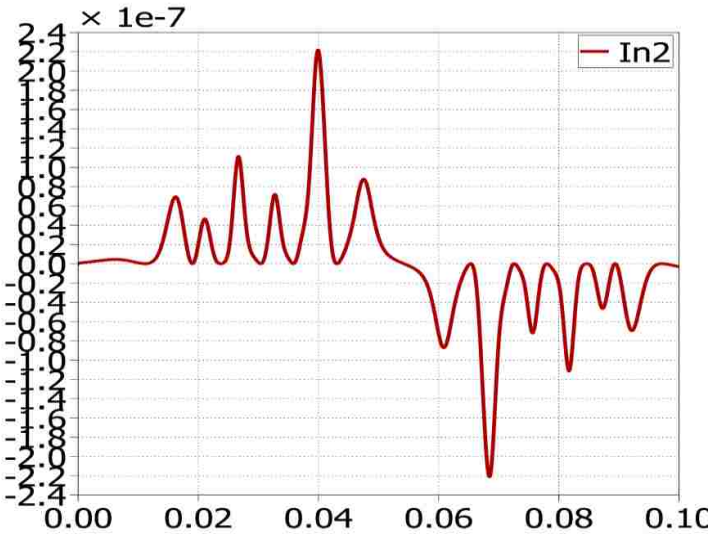

Figure 8.8: Force at the translator 2Hz reduced stroke length

Case-3: Full stroke length, speed =4 Hz

In this case the generator model is considered for full stroke length. But the speed of the translator is set at 4 Hz. Simulation time is same as in above two cases. For these conditions the output voltage, power and force waveforms are shown in Figures 8.9, 8.10 and 8.11 respectively. For the same time the translator will complete two cycles, i.e., two forward stokes and two reverse, as the speed of translator is twice as compared to the previous cases. Also the voltage and force gets doubled when compared to case 1 results because the velocity has doubled hence doubling the voltage and the force. As both voltage and current doubled, the power has increased by four times as compared to case 1.

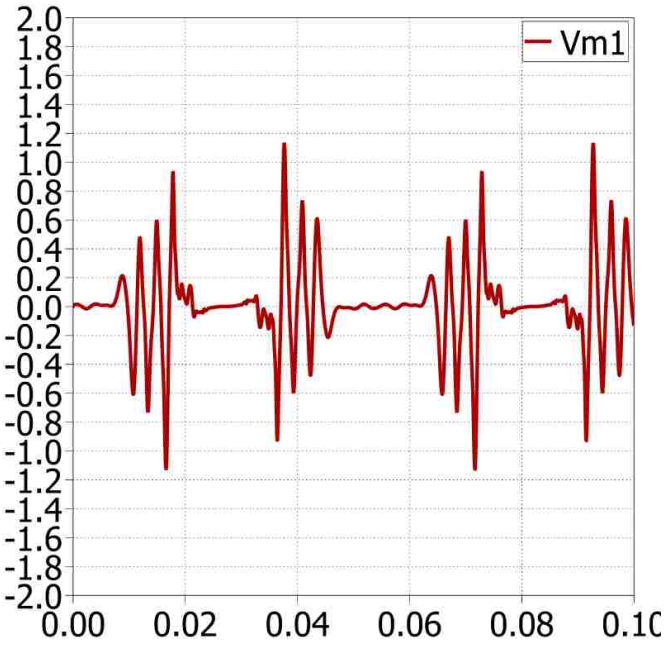

Figure 8.9: Terminal Voltage at 4Hz Full stroke length

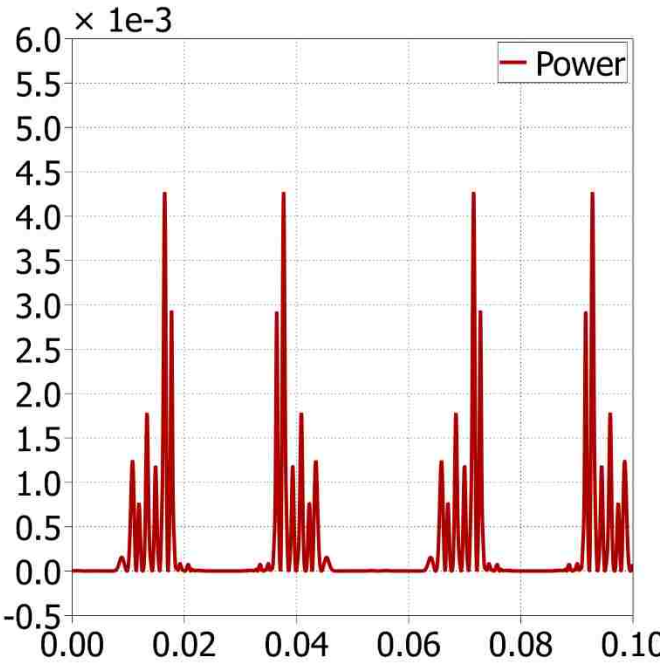

Figure 8.10: Output Power at 4Hz Full stroke length

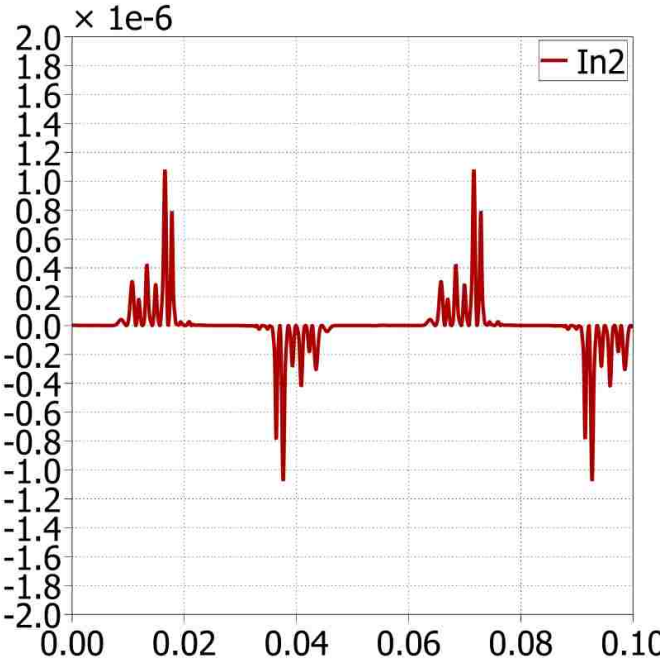

Figure 8.11: Force at the translator 4Hz Full stroke length

9. CONCLUSION

A TL-IPM generator has been simulated, built and tested. The practical results match well with the simulation results. The performance of the linear generator has been evaluated for various conditions using a Simulink model. The modeled generator performance matches the experiments. However, the induced voltage is small for all reasonable operating conditions. In future work, the design will be improved to generate more voltage. Also, a practical system could use several generators connected to a single VIV source to produce adequate energy. This approach, combined with methods to enhance VIV such as [9-10], can achieve practical energy extraction in a hydrokinetic system.

BIBLIOGRAPHY

[1] U.S. Environment Protection Agency. *Inventory of U.S. Greenhouse Gas Emissions And sinks: 1990-2008.*

[2] "Regulators Approve First Commercial Hydrokinetic Projects in the United States." *Today in Energy*. U.S. Energy Information Administration, 2 Oct. 2012.

[3] Jha, Alok. "'Wave Snakes' Switch on to Harness Ocean's Power." *The Guardian* [Manchester] 24 Sept. 2008.

[4]"How Hydrokinetic Energy Works." *Union of Concerned Scientists*. July 2008.

[5] Bernitsas, Michael M., Kamaldev Raghavan, Y. Ben-Simon, and E. M. H. Garcia. "VIVACE (Vortex Induced Vibration Aquatic Clean Energy): A New Concept in Generation of Clean and Renewable Energy From Fluid Flow." *Journal of Offshore Mechanics and Arctic Engineering* 130.4 (2008): 041101.

[6] P. Hew Wooi, H. Arof, and Wijono, "Design of a Permanent Magnet Linear Generator," in Proc. Strategic Technology, The 1st International Forum on, 2006, pp. 231-234.

[7] Benhama, A., A.c. Williamson, and A.b.j. Reece. "Force and Torque Computation from 2-D and 3-D Finite Element Field Solutions." *IEE Proceedings - Electric Power Applications* 146.1 (1999): 25.

[8] L. Szabo, C. Oprea, l. A. Viorel, and K. A. Biro, "Novel Permanent Magnet Tubular Linear Generator for Wave Energy Converters," in Proc. Electric Machines & Drives Conference, 2007. IEMDC '07. IEEE International, 2007, vol. 2, pp. 983-987.

[9] N. J. Baker, M. A. Mueller, and E. Spooner, "Permanent magnet air-cored tubular linear generator for marine energy converters," in Proc. Power Electronics, Machines and Drives, 2004. (PEMD 2004). Second International Conference on (Conf. Publ. No. 498), 2004, vol. 2, pp. 862-867 Vol.2.

[10] Bianchi, N., S. Bolognani, D. Dalla Corte, and F. Tonel. "Tubular Linear Permanent Magnet Motors: An Overall Comparison." *IEEE Transactions on Industry Applications* 39.2 (2003): 466-75.

[11] Hurd, Austin. *Optimizing the TL-IPM Design code*, internal report, Missouri University of Science and Technology, 2014.

[12] V.Lobo, N. Mainsah, A.Banerjee, J. W. Kimball, “Design feasibility of a vortex induced vibration based hydro-kinetic energy harvesting system,” *in Proceedings of the IEEE Green Technologies Conference*, 2011, EGST-7.

[13] A. Khalak and C. H. K. Williamson, "Fluid forces and dynamics of a hydroelastic structure with very low mass and damping," Journal of Fluids and Structures, vol. 11, pp. 973-982, November 1997.

[14] R. Govardhan and C. H. K. Williamson, "Resonance forever: existence of a critical mass and an infinite regime of resonance in vortex-induced vibration," Journal of Fluid Mechanics, vol. 473, pp. 147-166, 2002.

[15] A.Vinod, A.Kashyap, A.Banerjee, and J. Kimball, "Augmenting energy extraction from vortex induced vibration using strips of roughness/thickness combinations," in Proc. 1st Marine Energy Technology Symposium, 2013, pp.1-10.

[16] Jiabin Wang, G. W. Jewell and D. Howe, "A general framework for the analysis and design of tubular linear permanent magnet machines," in *IEEE Transactions on Magnetics*, vol. 35, no. 3, pp. 1986-2000, May 1999.doi: 10.1109/20.764898.

[17] Fair, Harry David. "Effect of the Magnetic Materiel on Railgun's Electromagnetic Field." *2012 16th International Symposium on Electromagnetic Launch Technology Conference Proceedings: Beijing, China, May 15-19, 2012*. Piscataway, NJ: IEEE, 2012.

VITA

Jamaluddin Mohammad was born in Hyderabad, India. In May 2012, he received a Bachelor of Science degree in Electrical and Electronics from Osmania University, Hyderabad, India. He was admitted into Missouri University of Science and Technology in January 2014 where he worked as a research assistant under Dr. Jonathan Kimball on the project 'Construction and Validation of TL-IPM Generator'. In December 2016 he received his MS degree in Electrical Engineering from Missouri University of Science and Technology, Rolla, Missouri, USA.